Fluid-phase behavior of binary mixtures in which one component can have two critical points

Swaroop Chatterjee and Pablo G. Debenedetti[a)]
Department of Chemical Engineering, Princeton University, Princeton, New Jersey 08544

(Received 10 February 2006; accepted 27 February 2006; published online 19 April 2006)

We investigate theoretically the binary fluid-phase behavior of mixtures in which one water-like component can have two critical points. We consider three equal-sized nonpolar solutes that differ in the strength of their dispersive interactions ($a_1 < a_2 < a_3$, where a denotes the van der Waals attractive parameter). In each case, we compare the phase behavior predicted using two sets of parameters for water: one giving rise to a pure component low-temperature liquid-liquid transition terminating at a critical point (two-critical-point parameter set), and one in which no such second critical point exists (singularity-free parameter set). Regardless of the parameter values used, we find five mixture critical lines. Using the two-critical-point parameter set, we find that a critical line originates at water's second critical point for aqueous mixtures involving solutes 1, 2, or 3. For mixtures involving solutes 1 or 2, this line extends towards low pressures and high temperatures as the solute mole fraction increases, and is closely related to the critical line originating at water's ordinary vapor-liquid critical point: these two critical lines are loci of upper and lower consolute points corresponding to the same liquid-liquid transition. In mixtures involving solute 2, the critical locus emanating from water's second critical point is shifted to higher temperatures compared to mixtures involving solute 1, and extends up to $T \approx 310$ K at moderate pressures (ca. 200 bars). This suggests the possibility of an experimentally accessible manifestation of the existence of a second critical point in water. For binary mixtures involving solutes 1 or 2, changing the water parameters from the two critical points to the singularity-free case causes the disappearance of a lower consolute point at moderate pressures. For binary mixtures involving solute 3, the differences between two-critical-point and singularity-free behaviors occur only in the experimentally difficult-to-probe low-temperature and high-pressure region. © *2006 American Institute of Physics*. [DOI: 10.1063/1.2188402]

I. INTRODUCTION

Understanding mixture phase behavior is of fundamental importance to the interpretation of geophysical phenomena associated with mineral formation, in geological exploration aimed at locating energy sources, in environmental science, and in the design of processes such as separations and materials processing with supercritical fluids.[1,2] The classic work of van Konynenburg and Scott[3,4] showed that the van der Waals equation of state with simple mixing rules can reproduce, with qualitative accuracy, a wide variety of experimentally observed mixture phase diagrams. One of the major achievements of Scott and van Konynenburg was to introduce the now widely used scheme for the classification of mixture phase behavior based on the (P,T) projections of critical lines and three-phase loci.[1–4] Subsequent extensions of their work have used other equations of state, including the Redlich-Kwong,[5] Carnahan-Starling[6]-Redlich-Kwong, perturbed-hard-chain,[7] and SAFT models[8–12] to compute mixture phase diagrams (see, e.g., Refs. 13–18). The resulting taxonomy of binary fluid-phase behavior has been particularly useful in the engineering design of high-efficiency separations in the oil and petrochemical industries.[1]

An important recent development in the subject of fluid-phase behavior has been the discovery of liquid-liquid equilibrium in pure substances. To date, this phenomenon has been found experimentally in phosphorus,[19] triphenyl phosphite,[20] and *n*-butanol.[21] Computer simulations of silicon,[22,23] silica,[24,25] and carbon[26] also show liquid-liquid transitions (but see Ref. 27 for recent computational evidence against a liquid-liquid transition in carbon). Such transitions usually (but not always[19]) occur at low temperatures, where liquid phases are metastable with respect to the stable crystal (i.e., they are supercooled). Accordingly, the phenomenology can also involve glassy states, and is often referred to as polyamorphism, occasionally also as polymorphism.[28,29] This latter terminology is to be avoided because the same term is widely used in the pharmaceutical physical chemistry literature to denote multiple crystal forms of the same compound.

Although intrinsically interesting as an unusual fluid-phase phenomenon, much of the current research activity on polyamorphism is a direct consequence of its possible relevance to supercooled and glassy water. The possibility that water may exhibit a liquid-liquid phase transition terminating at a metastable critical point has motivated a large body of experimental, computational, and theoretical research (for recent reviews, see Refs. 30 and 31). Interest in the physical

a)Electronic mail: pdebene@princeton.edu

properties of supercooled water has remained consistently high since the mid-1970s, following Speedy and Angell's pioneering work.[32] As first pointed out by these authors, many properties of water show a pronounced temperature dependence in the supercooled regime. Power-law fits to the isothermal compressibility, diffusion coefficient, viscosity, dielectric relaxation time, proton spin-lattice relaxation time, and oxygen spin-lattice relaxation time suggested an apparent singularity occurring at −45 °C, a few degrees below water's homogeneous nucleation temperature.[32] Analogous behavior was also found for the isobaric heat capacity[33–37] and the magnitude of the thermal expansion coefficient.[38,39]

Glassy water was first made in the laboratory some 70 years ago, by Burton and Oliver.[40] In 1985 Mishima *et al.* reported an apparently first-order phase transition between two forms of glassy water: high-density amorphous (HDA) and low-density (LDA) amorphous ices.[41] A few years later, in a pioneering paper, Poole *et al.* proposed what has come to be known as the second critical point (or liquid-liquid phase transition) scenario for the interpretation of the thermodynamic properties and global phase behavior of supercooled and glassy water.[42] According to this viewpoint, the transition between LDA and HDA is the structurally arrested manifestation of a first-order transition between two liquid phases of water: high-density liquid and low-density liquid (HDL and LDL). The transition terminates at a critical point, which is responsible for the experimentally observed increase in water's response functions upon supercooling. Thus, water is postulated to have two critical points: the ordinary vapor-liquid critical point and the metastable end point of the liquid-liquid transition. In the temperature range where the second critical point is thought to exist, liquid water is too cold not to crystallize upon supercooling and too hot not to crystallize upon heating across the glass transition. Accordingly, no direct observation of a liquid-liquid transition in supercooled water has been reported to date. Indirect evidence in support of the existence of a second critical point in water includes measurements of the melting curve of ice IV, showing abrupt changes in slope.[43,44] Such behavior implies, because of the Clausius-Clapeyron equation, a correspondingly abrupt change in the properties of the liquid phase. Computer simulations of the ST2 (Ref. 45) and TIP5P (Ref. 46) models of water have yielded clear evidence of a liquid-liquid transition.[47–50] Theoretical models of water also show liquid-liquid immiscibility at low temperatures and a second critical point.[51–55]

Recent computational work by Brovchenko *et al.* on several water models shows *multiple* liquid-liquid transitions[56,57] when density fluctuations are restricted so that the system remains homogeneous across the coexistence region.[58,59] The relationship between this interesting finding and the experimental identification of a third, apparently distinct, form of glassy water, namely, very high-density amorphous[60] (VHDA) ice is the subject of considerable current interest. In particular, it is not at present clear whether VHDA is simply a more stable form of HDA,[61–63] or whether it represents yet a new form of amorphous solid water. The latter possibility is of course consistent with the notion of multiple phase transitions (e.g., LDA-HDA and HDA-VHDA).

An alternative interpretation of the properties of supercooled water, known as the singularity-free scenario,[64,65] posits that the increase in water's response functions upon supercooling is the inevitable (thermodynamically consistent) result of the existence of a locus of density maxima with a negative slope in the (P,T) plane, and that such increases remain bounded. In this view, no low-temperature phase transition is needed to explain the experimental observations.

Investigating the phase behavior of binary mixtures in which one component can have two critical points is an interesting and important problem for two reasons. First, since polyamorphism has been experimentally observed in several liquids, it is natural to inquire how this added complexity in single-component phase behavior affects mixture phase diagrams. From this general liquid physics perspective, therefore, the objective is to extend the systematic investigation of mixture fluid-phase behavior pioneered by Scott and van Konynenburg to encompass the case in which one component can have more than one critical point.

Secondly, such an investigation may shed light into the metastable phase behavior of water. Here, one seeks to understand how the presence or absence of a metastable critical point in cold water affects the global phase behavior of binary aqueous mixtures. Recent experiments by Mishima on the LiCl-water system illustrate the usefulness of this approach.[66] The present work aims at providing currently lacking systematic understanding of the effects of a second critical point on mixture phase behavior. Though only a first step in this direction, the hope is that it may eventually be possible to deduce unambiguously the global phase behavior of pure water in the experimentally difficult-to-probe deeply supercooled region from that of its mixtures, possibly probed close to ambient conditions.

Theoretical models of water have been formulated which can exhibit both the two-critical-point and singularity-free behaviors through systematic variations in model parameters.[51–53] One of these models, due to Truskett *et al.*,[53] has been successfully extended to mixtures by Ashbaugh *et al.*,[67] and has been shown to reproduce key thermodynamic signatures associated with the hydrophobic hydration of small solutes.[67] This model is ideally suited for the present purposes, because it allows one to compare binary phase diagrams in the presence and in the absence of a second critical point in water. Furthermore, and regardless of the parameter set (singularity-free or two critical points), the model is able to reproduce water's distinctive equation-of-state anomalies, such as negative thermal expansion, increase in the isothermal compressibility upon cooling, and increase in the isobaric heat capacity upon cooling.[53]

In this study we use the Truskett-Ashbaugh model[67,68] to calculate the phase diagrams of three binary mixtures in which one component is a nonpolar solute and the other has waterlike properties. The three mixtures differ in the strength of the solute-solute dispersive interactions, and in each case we compare the predictions for the two-critical-point and singularity-free cases. Our goal is to uncover the classes of

TABLE I. Parameters for water model (Ref. 53).

	2-CP[a]	SF[b]
σ_w	3.11 Å	3.11 Å
r_{wi}	$1.01\sigma_w$	$1.005\sigma_w$
r_{wo}	$1.04\sigma_w$	$1.03\sigma_w$
a_{ww}	0.269 Pa m^6/mol^2	0.269 Pa m^6/mol^6
ϕ^*	0.175 rad	0.16 rad
$\epsilon_{\max}$	23 kJ/mol	23 kJ/mol
ϵ_{pen}	3 kJ/mol	3 kJ/mol
$j_{\max}$	8	8

[a]Two-critical-point parameter set.
[b]Singularity-free parameter set.

global phase behavior that may arise in a binary mixture when one component has two critical points. At this stage, generic investigations of phase behavior, eventually leading to a Scott and van Konynenburg-type taxonomy, are more important than quantitatively accurate predictions for specific aqueous mixtures.

Clearly, in light of recent results suggesting the existence of multiple metastable liquid-liquid transitions,[56,57] the present investigation must be regarded as the initial step in the study of the relationship between pure component polyamorphism and mixture phase behavior. In this sense, what we consider here is the simplest case in which one component can have *just* two critical points. Furthermore, we consider here only the effects of varying the strength of solute-solute interactions. Work is currently in progress on a systematic investigation of the effects of solute size (in addition to dispersive interactions) on mixture phase behavior, and results will be reported in separate publications.

This paper is structured as follows. In Sec. II we review the Truskett-Ashbaugh model. The calculation of phase hase boundaries, stability limits, and critical lines is discussed in Sec. III. Section IV presents the calculated phase diagrams. The main conclusions from this study, as well as suggestions for future work along these lines, are contained in Sec. V.

II. MICROSCOPIC MODEL

Here, we provide a brief description of the statistical mechanical model for the model of water, first introduced by Truskett *et al.*,[53] and later extended to mixtures by Ashbaugh *et al.*[67] Details of the derivation and discussion can be found in the original references. The central quantity is the canonical partition function of a mixture of N_w water molecules and N_s solute molecules in a volume V at temperature T, given by

$$Q(N_w,N_s,V,T)=\left(\frac{1}{N_w!N_s!\Lambda_w^{3N_w}\Lambda_s^{3N_s}}\right)\times(V-Nb)^N\exp(N\beta\rho a)(4\pi)^{N_w}\times\prod_{j=1}^{j_{\max}}\prod_{k=0}^{k_{\max}}f_{j,k}^{N_w p_{j,k}}. \quad (1)$$

Here, Λ_i denotes the thermal wavelength of component i; $N=N_w+N_s$, the total number of molecules; $\beta^{-1}=k_BT$, the product of Boltzmann's constant and the temperature. The van der Waals attractive interaction and excluded volume terms for the mixture, given by a and b, respectively, were computed using standard mixing rules,

$$a=x_w^2a_{ww}+2x_wx_sa_{sw}+x_s^2a_{ss}, \quad (2a)$$

$$b=x_wb_w+x_sb_s, \quad (2b)$$

where $x_i=N_i/N$ is the mole fraction of component i and the cross solute-water van der Waals interaction parameter is given by $a_{sw}=\sqrt{a_{ww}a_{ss}}$. The pure component excluded volume parameters are determined by the individual component van der Waals diameters, σ_i, so that the pressure diverges at the random close packing density $0.64b_i=\pi\sigma_i^3/6$, where the spheres occupy 64% of the volume. Equation (2b) is the usual van der Waals mixing rule for molecular volumes. In the future, it would be interesting to investigate the additivity of diameters instead of volumes.

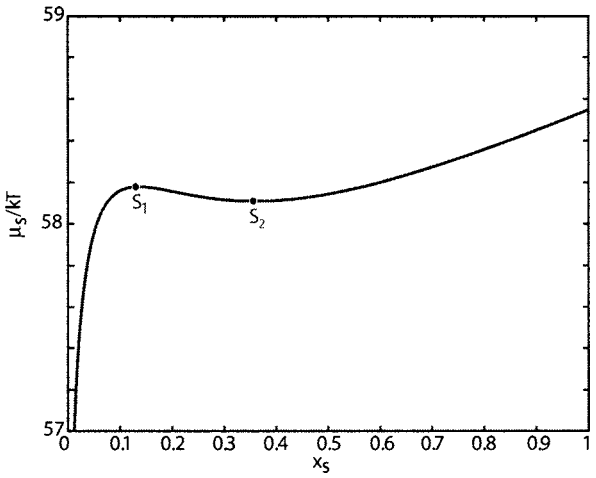

FIG. 1. μ_s-x_s plot for solute 1 (see Table II) at $P=3$ kbars and $T=400$ K employing the two-critical-point scenario parameters for water (see Table I). S_1 and S_2 are the two spinodal points.

The partition function defined in Eq. (1) is a perturbation of the classical van der Waals model wherein the contribution of orientation-dependent hydrogen bonding is included. Water molecules possess a hard core of radius σ_w. In order to form a hydrogen bond, a water molecule i, also referred to as the *central* water molecule, must be surrounded by an *exclusion shell* of radius r_{wi}, devoid of centers of other water molecules, and a second water molecule j must be located within molecule i's *hydrogen bonding shell* $r_{wi}\leqslant r\leqslant r_{wo}$. In addition, molecules i and j must be properly oriented with respect to each other. The presence of additional water molecules within i's hydrogen bonding shell weakens the bond between i and j. Solute molecules also possess a hard core of radius σ_s, hence no solute molecule can penetrate within a sphere of radius $\sigma_{sw}=(\sigma_w+\sigma_s)/2$ around a water molecule. In order to form a hydrogen bond with another water molecule in the presence of solutes, molecule i must also be surrounded by a solute exclusion shell of radius r_{si}. Solute molecules whose centers lie within the central water molecule's *hydration shell* ($r_{si}\leqslant r\leqslant r_{so}$) can in principle either strengthen or weaken a hydrogen bond. In this work, however, we take $r_{si}=r_{so}=\sigma_{sw}$, which means that solute molecules cannot affect the strength of an existing hydrogen bond.

The quantity $p_{j,k}$ in Eq. (1) is the probability that j water molecules and k solute molecules occupy the hydrogen bonding shell of a given water molecule whose exclusion shells are devoid of both water and solute molecules. It is computed from hard-sphere statistics and hence depends only on density and composition, but not on temperature. Detailed expressions are given in Ref. 67. The quantity $f_{j,k}$ is the central water molecule's orientational contribution to its hydrogen bonding partition function, and is given by

$$f_{j,k} = 1 + \frac{j}{4}(1 - \cos\phi^*)^2(e^{\beta\epsilon_{j,k}} - 1), \tag{3}$$

where ϕ^* is a critical angle for hydrogen bonding, such that the bonding vectors of two water molecules must form angles ϕ_1, $\phi_2 < \phi^*$ with respect to the line joining their centers in order for a hydrogen bond to form. In Eq. (3), $\epsilon_{j,k}$ is the energy associated with the formation of a hydrogen bond between two water molecules,

$$-\epsilon_{j,k} = -\epsilon_{\max} + (j-1)\epsilon_{\text{pen}}, \tag{4}$$

where $(j-1)$ denotes the number of crowding water molecules that weaken the hydrogen bond, ϵ_{pen} is the energetic penalty due to the presence of a crowding molecule within molecule i's hydrogen bonding shell, and $\epsilon_{\max}$ is the maximum strength of a hydrogen bond. The above equation can, in general, incorporate an energy penalty term due to the presence of k nonpolar solutes in the hydrogen bonding shell. As explained above, however, we consider the situation, as was done in Refs. 67 and 68, in which solute molecules have no effect on hydrogen bond strength. Table I lists the water parameters used in this work. One set of parameters, denoted 2-CP, gives rise to a low-temperature liquid-liquid phase transition and a second critical point. The other set, denoted SF, reproduces the singularity-free scenario,[64,65] in which water has only the ordinary vapor-liquid critical point.

The equation of state and solute and water chemical potentials are obtained by straightforward differentiation of the partition function, and are given by

$$P = \frac{\rho k_B T}{1-\rho b} - a\rho^2 + N_w k_B T \sum_{j=1}^{j_{\max}} \sum_{k=0}^{k_{\max}} \left(\frac{\partial p_{j,k}}{\partial V}\right)_{T,N_w,N_s} \ln f_{j,k}, \tag{5}$$

$$\mu_s = \left(\frac{\partial A}{\partial N_s}\right)_{T,V,N_w} = -k_B T\left(\frac{\partial \ln Q}{\partial N_s}\right)$$

$$= k_B T \ln \rho_s \Lambda_s^3 - k_B T \ln(1-\rho b) + \frac{k_B T \rho b_s}{1-\rho b} - 2(\rho_w a_{sw} + \rho_s a_{ss}) - k_B T \rho_w \sum_{j=1}^{j_{\max}} \sum_{k=0}^{k_{\max}} \left\{ \left[\frac{\partial p_{j,k}}{\partial \rho_s}\right]_{\rho_w} \ln f_{j,k} \right\}, \tag{6}$$

and

$$\mu_w = \left(\frac{\partial A}{\partial N_w}\right)_{T,V,N_s} = -k_B T\left(\frac{\partial \ln Q}{\partial N_w}\right)$$

$$= k_B T \ln \rho_w \Lambda_w^3 - k_B T \ln(1-\rho b) + \frac{k_B T \rho b_w}{1-\rho b} - 2(\rho_w a_{ww} + \rho_s a_{sw}) - k_B T \rho_w \sum_{j=1}^{j_{\max}} \sum_{k=0}^{k_{\max}} \left\{ \left[\frac{\partial p_{j,k}}{\partial \rho_w}\right]_{\rho_s} \ln f_{j,k} \right\}$$

$$- k_B T \sum_{j=1}^{j_{\max}} \sum_{k=0}^{k_{\max}} p_{j,k} \ln f_{j,k}. \tag{7}$$

III. CALCULATION METHODS

To generate phase diagrams we fix P and T, and we calculate solute and water chemical potentials (μ_s, μ_w) as a function of composition (x_s). This requires solving for ρ using Eq. (5), and then using Eqs. (6) and (7). From this we generate a $\mu_s(x_s)$ curve, such as the one shown in Fig. 1. Extrema in such a curve correspond to limits of stability. Two such spinodal points, S_1 and S_2, are shown in Fig. 1.

The conditions of equilibrium for two coexisting phases I and II are given by

$$P_{\text{I}} = P_{\text{II}}, \tag{8}$$

$$T_{\text{I}} = T_{\text{II}}, \tag{9}$$

$$\mu_{s,\text{I}} = \mu_{s,\text{II}}, \tag{10}$$

$$\mu_{w,\text{I}} = \mu_{w,\text{II}}. \tag{11}$$

A convenient way of finding solutions to these equations is to cross-plot μ_s versus μ_w. The points of intersection correspond to phase coexistence. This is illustrated in Fig. 2, which shows the μ_s versus μ_w plot corresponding to Fig. 1. Numerical convergence is achieved by first picking an estimate of the coexistence chemical potential (say for μ_s) in the vicinity of the point of intersection on the μ_s versus μ_w plot. Using the corresponding estimate of the coexistence compositions for the two phases, the chemical potentials for water (μ_w) at the same mole fractions are compared. The differ-

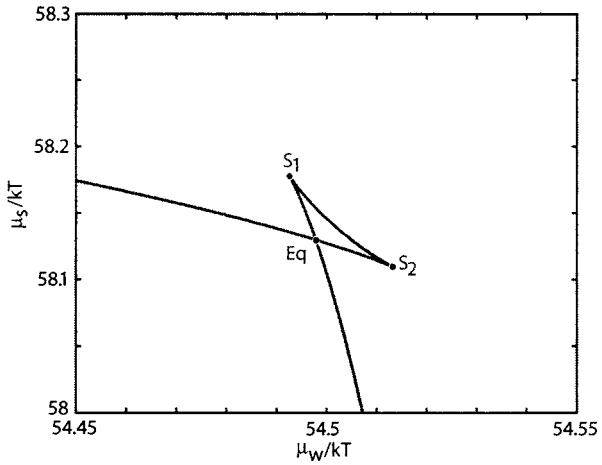

FIG. 2. μ_s-μ_w plot for solute 1 (see Table II) at $P=3$ kbars and $T=400$ K employing the two-critical-point scenario parameters for water (see Table I). S_1 and S_2 are the two spinodal points. "Eq" represents the equilibrium coexistence point for the two binary phases with S_1 and S_2 as limits of stability.

ence between the two water chemical potential values is then minimized by iterating on the solute chemical potential. In all of the calculations reported here, convergence was considered to occur when the relative change in the chemical potential of water in each phase between successive iterations fell below one part in 10^5.

Once an estimate for the location of a mixture critical point was obtained from the merging of spinodals in a μ_i versus x_i plot, a precise calculation was performed by solving the binary mixture criticality conditions[69]

$$A_{ss}A_{ww} - A_{sw}^2 = 0, \tag{12}$$

$$A_{www}A_{ss}^2 - A_{sss}A_{ww}A_{sw} - 3A_{sww}A_{ss}A_{sw} + 3A_{ssw}A_{ss}A_{ww} = 0. \tag{13}$$

In the above equations, both of which must be satisfied simultaneously at a critical point, A denotes the Helmholtz energy ($=-k_BT\ln Q$), and subscripts s and w denote differentiation with respect to N_s and N_w, respectively. Pure component binodal curves were obtained from the respective equations of state, that is to say the van der Waals equation for the solute and the model of Truskett *et al.*[53] for water.

IV. RESULTS AND DISCUSSION

Table II lists the hard-core diameters and van der Waals attractive parameters of the three solutes considered in this work. Neglecting the association term in the partition function, the model reduces to a van der Waals mixture. The three mixtures considered here would then correspond to types III (solute 1) and II (solutes 2 and 3) in the Scott and van Konynenburg classification.

TABLE II. Solutes used in phase equilibrium calculations.

Solute	σ_{ss} (Å)	a_{ss} (Pa m^6/mol^2)
1	4	0.2
2	4	0.26
3	4	0.4

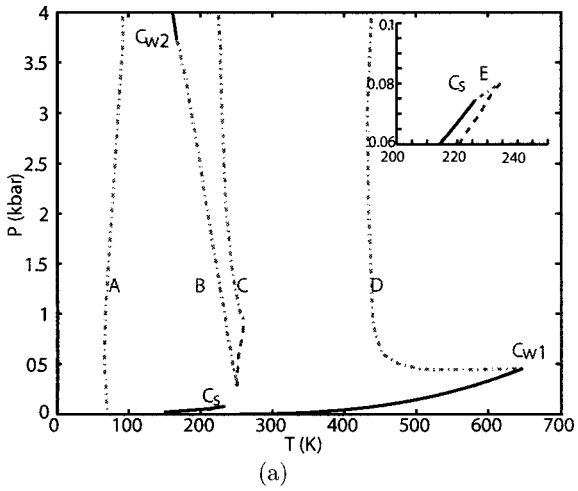

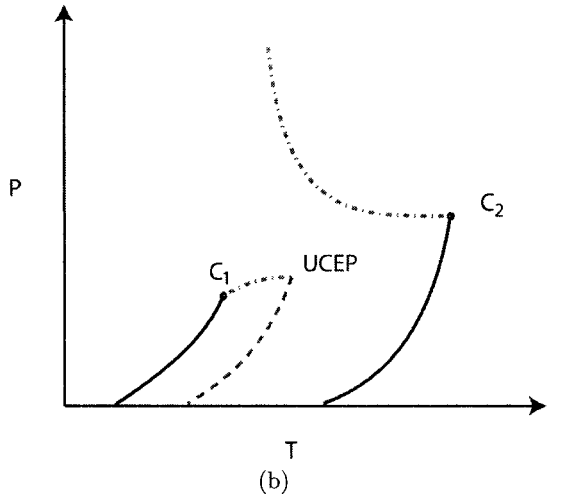

FIG. 3. (a) P-T projection of the fluid-phase behavior for a binary aqueous mixture of solute 1 (see Table II), using the two-critical-point scenario parameter set for water (see Table I). Solid lines indicate pure component phase coexistence lines; dot-dashed lines, binary mixture critical lines; dashed lines, triple point lines. A, B, C, D, and E (in inset) are binary mixture critical lines. C_{w1} and C_{w2} are the vapor-liquid and liquid-liquid critical points of water, respectively. C_s is the vapor-liquid critical point of the solute. (b) Schematic representation of Type III phase behavior based on the classification of Scott and van Konynenburg (Refs. 3 and 4) for a binary mixture of components 1 and 2 with vapor-liquid critical points C_1 and C_2. UCEP is an upper critical end point.

Figure 3(a) shows the (P,T) projection of the phase diagram for solute 1, using the two-critical-point parameters for water (Table I). There are five critical lines, three of which, D, B, and E, originate at the pure component critical points. Lines D and E, originating at the vapor-liquid critical points of water and the solute, respectively, are consistent with type III behavior [Fig. 3(b)]. In particular, critical line D, emanating from the less volatile component's vapor-liquid critical point, traces towards high pressures, while critical line E ends at an upper critical end point (UCEP). A three-phase (LLV) line extends from the UCEP to lower temperatures and pressures. The other critical loci, A and C, correspond to upper critical points of two separate liquid-liquid transitions. Figure 4 shows a (T,ρ) projection of the phase diagram of this mixture, at 3 kbars. It can be seen that the two critical loci originating at water's vapor-liquid and liquid-liquid criti-

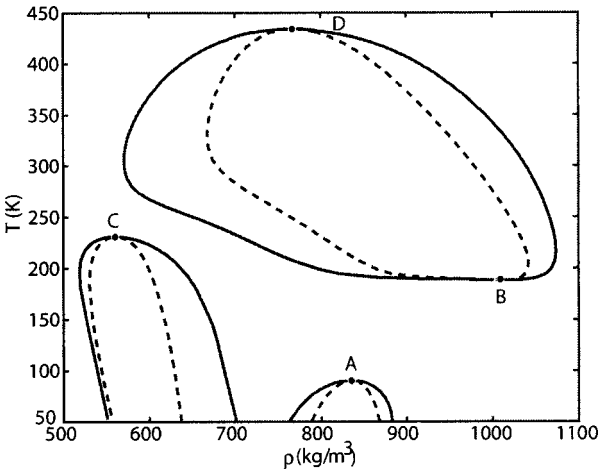

FIG. 4. T-ρ projection of the fluid-phase behavior at $P=3$ kbars for a binary aqueous mixture of solute 1 (see Table II), using the two-critical-point scenario parameter set (see Table I). Solid lines indicate binodal curves, while dashed lines are spinodal curves. A, B, C, and D are critical points (●) that lie on critical lines denoted by the same letter in Fig. 3(a).

cal points (D and B, respectively) are lines of upper and lower end points corresponding to the same phase transition. This means that in the presence of a second component there appears a closed-loop immiscibility region linking water's two critical points. As the pressure decreases, the binodal curves corresponding to critical points B and C approach each other until, eventually, the two envelopes merge, giving rise to a fluid-fluid-fluid triple point. This is shown in Fig. 5. The resulting triple point line is shown in Fig. 3(a), connecting the critical loci B and C.

The calculated phase behavior for solute 1, using the singularity-free parameters for water (Table I) is shown in Fig. 6. It is interesting to compare this (P,T) projection with the corresponding two-critical-point case [Fig. 3(a)]. It can be seen that there are still five critical loci, two of which

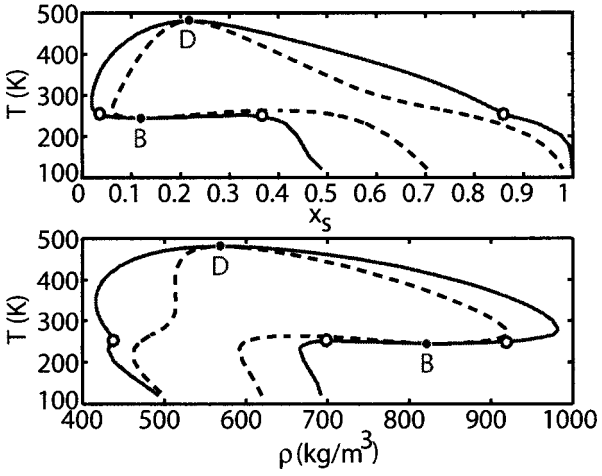

FIG. 5. T-x_s (top) and T-ρ (bottom) projections of the fluid-phase behavior at $P=0.5$ kbar for a binary aqueous mixture of solute 1 (see Table II), using the two-critical-point scenario parameter set (see Table I). Solid lines indicate binodal curves, while dashed lines are spinodal curves. B and D are critical points (●) that lie on critical lines denoted by the same letter in Fig. 3(a). (○) denotes three coexistence phases at $T=253$ K. This represents one point along the dashed locus of fluid triple points joining the critical lines B and C in Fig. 3(a).

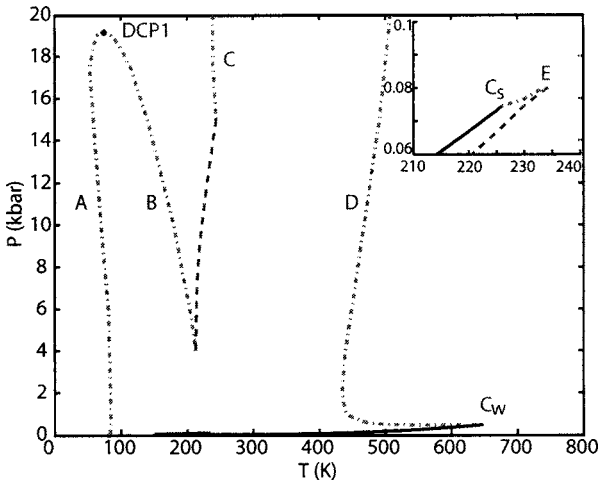

FIG. 6. P-T projection of the fluid-phase behavior for a binary aqueous mixture of solute 1 (see Table II), using the singularity-free scenario parameter set for water (see Table I). Solid lines indicate pure component phase coexistence lines; dot-dashed lines, binary mixture critical lines; dashed lines, triple point lines. A, B, C, D, and E (in inset) are binary mixture critical lines. C_w and C_s are the vapor-liquid critical points for water and solute 1, respectively. DCP1 is a double critical point where, along a critical locus, $\partial P/\partial T|_c=0$.

(D,E) behave very similarly in both cases, and hence are not sensitive to the presence of a second critical point in water. Critical loci D and B are still, as in the two-critical-point case, upper and lower end points of a common phase transition. However, in the absence of a second critical point, critical lines B and C are displaced towards high pressures. Critical lines A and B merge at a double critical point[70] (DCP1 in Fig. 6).

Figure 7(a) shows the (P,T) projection of the phase diagram for solute 2, using the two-critical-point parameters for water (Table I). As was found to be the case for mixture 1, there are five critical lines. Lines E, which joins the two vapor-liquid critical points, and D, are consistent with type II phase behavior [Fig. 7(b)]. In particular, a locus of triple points ends at an UCEP, from which critical line D extends towards the high-pressure region. Lines A, B, and C are a consequence of the association term in the equation of state. Of these, line A is a locus of upper critical points associated with a low-temperature liquid-liquid transition. As was found to be the case for mixture 1, critical line B, which originates at water's second critical point, and C terminate at low pressures at the end points of a line of triple points. This is shown in detail in Fig. 7(c). The crossing of lines B and C around 2 kbars is shown in detail in Figs. 8(a) and 8(b). It can be seen that these are independent transitions, with $T_c(C) > T_c(B)$ at 3 kbars [Fig. 8(a)] and $T_c(B) > T_c(C)$ at 1 kbar [Fig. 8(b)]. Similarly to the case of mixture 1, there is a broad region of closed-loop immiscibility, of which lines D and B are the upper and lower end point loci, respectively. However, line D does not originate at water's vapor-liquid critical point. Interestingly, the added attractions (solute 2 versus solute 1, see Table II) shift the low-pressure, high-temperature portion of critical line B, which emanates from water's metastable critical point, towards the experimentally accessible region (e.g., 300 K, 300 bars).

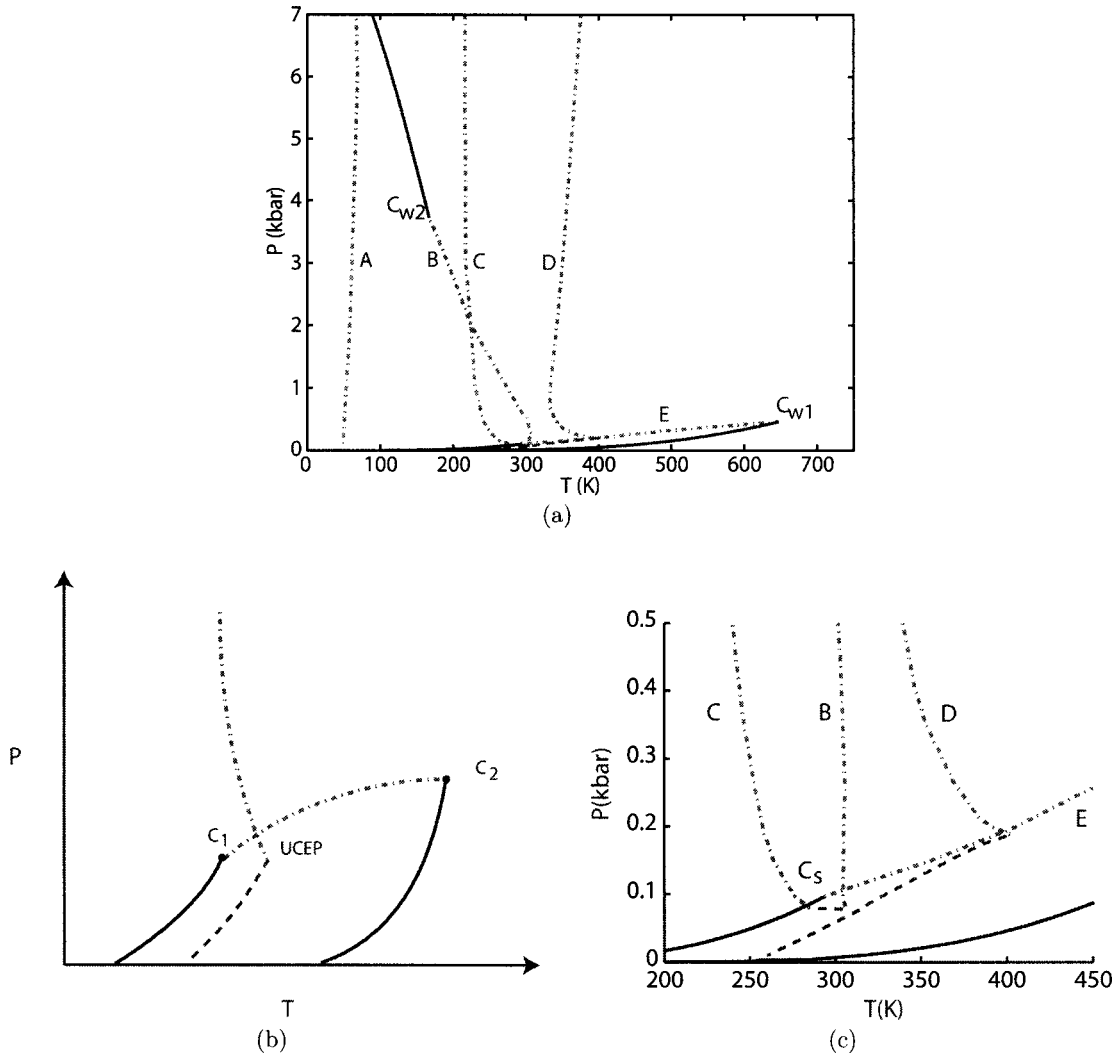

FIG. 7. (a) *P-T* projection of the fluid-phase behavior for a binary aqueous mixture of solute 2 (see Table II), using the two-critical-point scenario parameter set for water (see Table I). Solid lines indicate pure component phase coexistence lines; dot-dashed lines, binary mixture critical lines; dashed lines, triple point lines. *A*, *B*, *C*, *D*, and *E* (in inset) are binary mixture critical lines. C_{w1} and C_{w2} are the vapor-liquid and liquid-liquid critical points of water, respectively. C_s is the vapor-liquid critical point of the solute. (b) Schematic representation of Type II phase behavior based on the classification of Scott and van Konynenburg (Refs. 3 and 4) for a binary mixture of components 1 and 2 with vapor-liquid critical points C_1 and C_2. UCEP is an upper critical end point. (c) A detailed view of the phase behavior in the vicinity of the solute's critical point (C_s).

The corresponding singularity-free behavior for this mixture is shown in Figs. 9(a) and 9(b). Once again, there are five critical loci. Comparison with Fig. 7 shows that in the absence of water's second critical point, lines *B* and *C* are displaced towards high pressures. In analogy with the singularity-free case for mixture 1 (Fig. 6), critical loci *A* and *B* merge at a high-pressure double critical point.

Figure 10 shows the (P,T) projection of the phase diagram for solute 3, using the two-critical-point parameters for water (Table I). The added attractions (solute 3 versus solutes 2 and 1, see Table II) cause a qualitative change in critical line *B*. Starting from water's metastable critical point, where this critical line originates, there is now a comparatively narrow range of temperatures and pressures within which locus *B* has a negative slope. There is also a correspondingly narrow window of pressures and temperatures within which closed-loop immiscibility occurs. Critical lines *D* and *B*, upper and lower end points of this phase transition, merge at a double critical point (DCP2 in Fig. 10). Figure 11 shows a (T,x_s) projection at 3500 bars. It can be seen that both liquid phases whose coexistence terminates at critical point *C* are solute rich, whereas the closed-loop immiscibility region is also very narrow in terms of solute mole fraction, both coexisting phases containing less than 10% (mole) of solute. Even though this mixture would correspond to type II behavior (Table II), the association contributions distort one aspect of type II behavior significantly. Critical line *D* does not end at an UCEP at low pressures (compare with Fig. 7), but instead it merges with line *B* at the above-mentioned double critical point.

The corresponding singularity-free behavior for this mixture is shown in Fig. 12. Comparison with Figs. 6 and 9 (singularity-free water+solute 2 and 3, respectively) reveals a qualitative change in phase behavior brought about by the stronger solute-solute dispersive attractions (Table II). The line of triple points linking critical lines *B* and *C* has disappeared; instead, critical line *B*, as in the two-critical-point case (Fig. 10), spans a very narrow range of temperatures

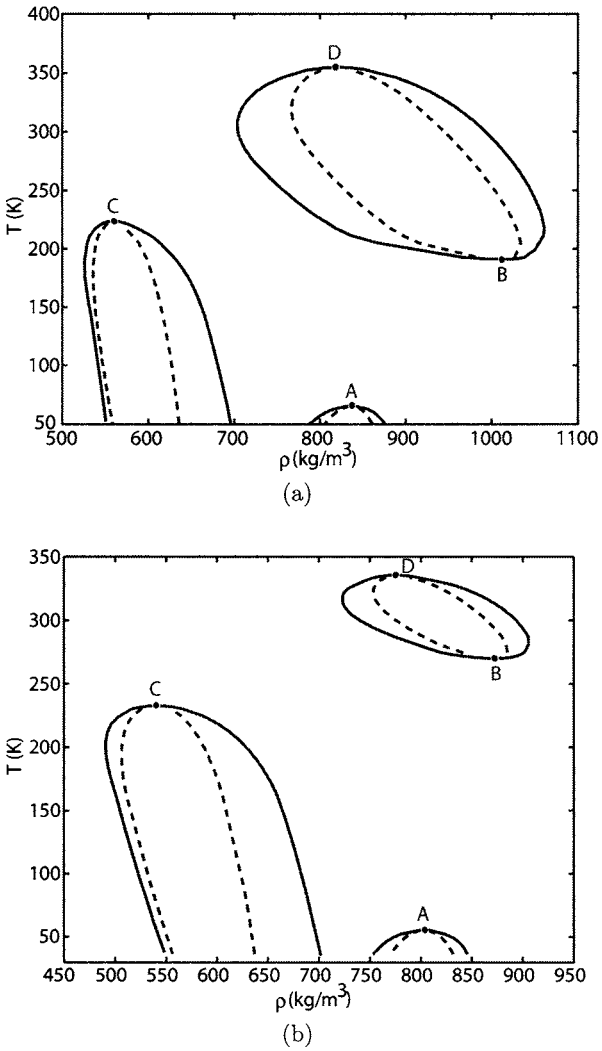

FIG. 8. T-ρ projection of the fluid-phase behavior at (a) $P=3$ kbars and (b) at $P=1$ kbar for a binary aqueous mixture of solute 2 (see Table II), using the two-critical-point scenario parameter set for water (see Table I). Solid lines indicate binodal curves, while dashed lines are spinodal curves. A, B, C, and D are critical points (●) that lie on critical lines denoted by the same letter in Fig. 7(a). Note that the temperatures corresponding to critical points B and C are such that $T_c(C)>T_c(B)$ at 3 kbars, but $T_c(B)>T_c(C)$ at 1 kbar. This is reflected in the crossing of critical lines B and C in Fig. 7(a).

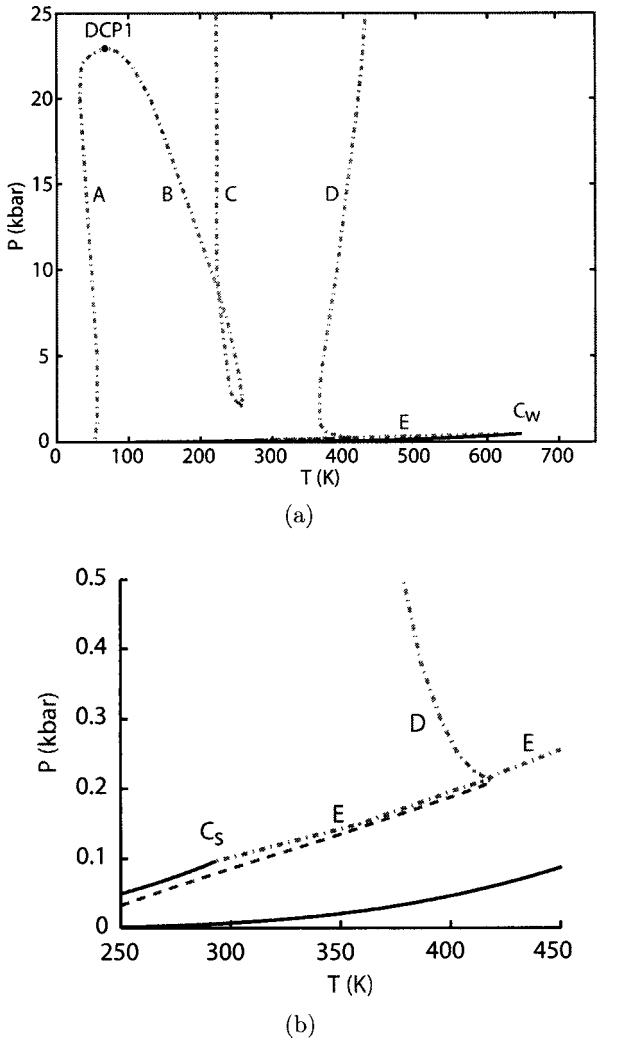

FIG. 9. (a) P-T projection of the fluid-phase behavior for a binary aqueous mixture of solute 2 (see Table II), using the singularity-free scenario parameter set for water (see Table I). Solid lines indicate pure component phase coexistence lines; dot-dashed lines, binary mixture critical lines; dashed lines, triple point lines. A, B, C, D, and E (in inset) are binary mixture critical lines. C_w and C_s are the vapor-liquid critical points for water and solute 2, respectively. DCP1 is a double critical point where, along a critical locus, $\partial P/\partial T|_c=0$. (b) A detailed view of the phase behavior in the vicinity of the solute's critical point (C_s).

and pressures bound here by double critical points DCP1 and DCP2, and by DCP2 and water's second critical point in the two-critical-point scenario. Accordingly, the immiscibility region with upper and lower critical points (D and B, respectively) is restricted to a narrow range of temperatures and pressures bound by DCP1 (higher-pressure, lower-temperature limit) and DCP2 (lower-pressure, higher-temperature limit).

V. CONCLUSIONS

In this work we have investigated theoretically the binary fluid-phase behavior of mixtures in which one component can have two critical points. The three equal-sized nonpolar solutes considered differ by the strength of dispersive interactions. Neglecting the hydrogen bonding terms in the partition function, the model reduces to a van der Waals mixture, and the cases considered here would then correspond to type III (solute 1) and type II (solutes 2 and 3) mixtures in the Scott and van Konynenburg classification.[3,4] In each case, we compare the phase behavior predicted by using the two-critical-point and the singularity-free parameters for the waterlike component. Regardless of the parameter values used, we find five mixture critical lines. Locus A is a low-temperature liquid-liquid transition; locus B originates at water's second critical point (two-critical-points parameter set) or at a high-pressure double critical point where it merges with A (singularity-free parameter set). Locus C occurs in the 200–250 K range for all cases studied. Locus D originates at water's vapor-liquid transition. Locus E originates at the solute's critical point, and either forms a continuous line joining it to water's vapor-liquid critical point (solutes 2 and 3) or ends at an upper critical end point where it intersects a line of fluid triple points.

Using the two-critical-point parameter set for water, we

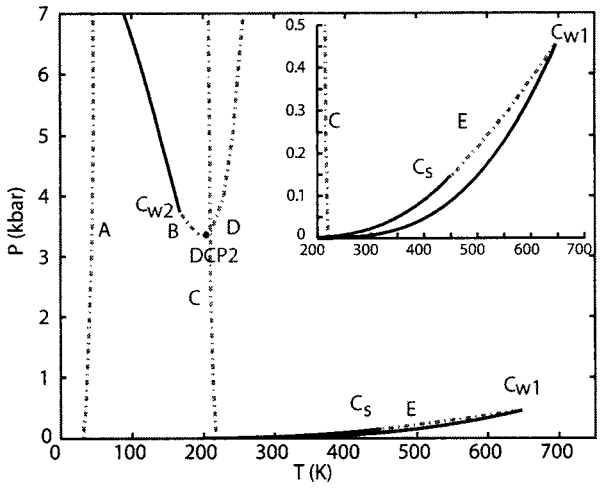

FIG. 10. *P-T* projection of the fluid-phase behavior for a binary aqueous mixture of solute 3 (see Table II), using the two-critical-point scenario parameter set for water (see Table I). Solid lines indicate pure component phase coexistence lines; dot-dashed lines, binary mixture critical lines; dashed lines, triple point lines. *A*, *B*, *C*, *D*, and *E* (in inset) are binary mixture critical lines. C_{w1} and C_{w2} are the vapor-liquid and liquid-liquid critical points of water, respectively. C_s is the vapor-liquid critical point of the pure solute. DCP2 is a double critical point where, along a critical locus, $\partial P/\partial T|_c=0$.

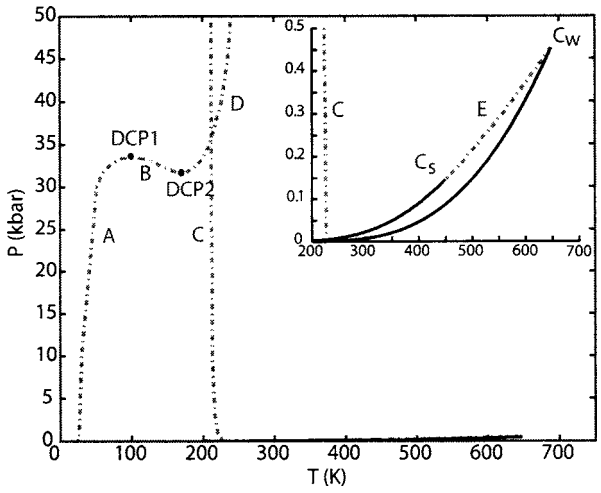

FIG. 12. *P-T* projection of the fluid-phase behavior for a binary aqueous mixture of solute 3 (see Table II), using the singularity-free scenario parameter set for water (see Table I). Solid lines indicate pure component phase coexistence lines; dot-dashed lines, binary mixture critical lines. *A*, *B*, *C*, *D*, and *E* (in inset) are binary mixture critical lines. C_w and C_s are the vapor-liquid critical points for water and solute 3, respectively. DCP1 and DCP2 are double critical point where, along a critical locus, $\partial P/\partial T|_c=0$.

find that a critical line originates at water's second critical point for aqueous mixtures involving any of the three solutes considered. For mixtures involving either solute 1 or solute 2 this line extends towards low pressures and high temperatures as the solute mole fraction increases, and is closely related to the critical line originating at water's ordinary vapor-liquid critical point: these two critical lines are loci of upper and lower consolute points corresponding to the same liquid-liquid transition. A notable effect of stronger solute-solute attractions upon going from solute 1 to solute 2 is to shift the critical locus emanating at water's second critical point towards higher temperatures. Specifically, this locus extends up to $T\approx 310$ K at moderate pressures (ca. 200 bars), suggesting the possibility of an experimentally accessible manifestation of the existence of a second critical point in water's deeply supercooled region.

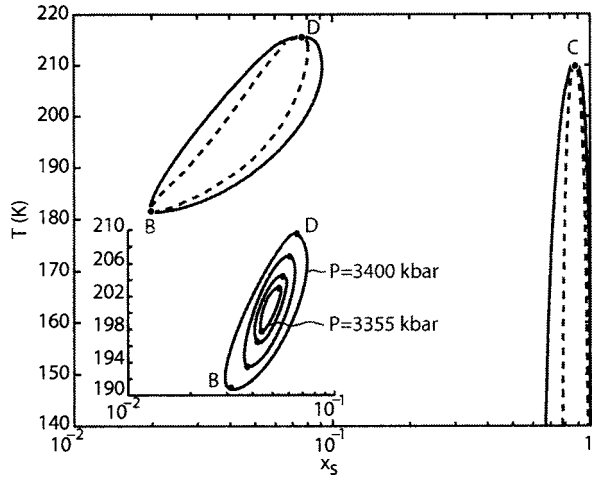

FIG. 11. *T*-x_s projection of the fluid-phase behavior at $P=3500$ bars for a binary aqueous mixture of solute 3 (see Table II), using the two-critical-point scenario parameter set for water (see Table I). Solid lines indicate binodal curves, while dashed lines are spinodal curves. *B*, *C*, and *D* are critical points (●) that lie on critical lines denoted by the same letter in Fig. 10. The inset shows how DCP1 is formed due to the merging of critical loci *B* and *D*. As the pressure decreases, critical points *B* and *D* approach each other, finally coinciding at a DCP.

For binary mixtures involving solutes 1 or 2, changing the water parameters from the two critical points to the singularity-free case causes a marked shift towards high pressures in critical lines *B* and *C*. Thus in both cases the difference between the mixture phase behavior in the presence and in the absence of a second critical point for water is the absence (singularity free) or presence (two critical points) of a lower consolute point (*B*) at moderate pressures. For binary mixtures involving solute 3, the differences between two-critical-point and singularity-free behaviors occur only in the experimentally difficult-to-probe low-temperature and high-pressure region.

The present work is an initial step in the direction of a systematic exploration of mixture phase behavior in which one component exhibits polyamorphism. Here we have considered the effects of solute-solute attractions on mixture phase behavior. We plan to investigate the influence of solute size and to perform similar calculations with other models exhibiting polyamorphism. Model refinement to include more complex solutes (e.g., ions, polar molecules) is another interesting avenue for future investigations. The ultimate goal of this work is twofold. We aim at a taxonomy of mixture fluid-phase behavior in the presence of polyamorphism. We also want to apply such a systematic understanding to eventually suggest measurements that can confirm or refute the existence of a second critical point in water and that involve stable phases at near-ambient temperatures and pressures.

ACKNOWLEDGMENTS

P.G.D. gratefully acknowledges the support of the Department of Energy, Division of Chemical Sciences, Geosciences and Biosciences, Office of Basic Energy Sciences, Grant No. DE-FG0287ER13714, and of the National Science Foundation through Collaborative Research in Chemistry Grant No. CHE 0404699.

[1] J. S. Rowlinson and F. L. Swinton, *Liquids and Liquid Mixtures*, 3rd ed. (Butterworth Scientific, London, 1982).
[2] J. Prausnitz, R. Lichtenthaler, and E. Gomes de Azevedo, *Molecular Thermodynamics of Fluid-Phase Equilibria*, 3rd ed. (Prentice-Hall, Upper Saddle River, NJ, 1999).
[3] P. H. van Konynenburg and R. L. Scott, Philos. Trans. R. Soc. London, Ser. A **298**, 495 (1980).
[4] R. L. Scott and P. H. van Konynenburg, Discuss. Faraday Soc. **49**, 87 (1970).
[5] O. Redlich and J. Kwong, Chem. Rev. (Washington, D.C.) **44**, 233 (1949).
[6] N. Carnahan and K. E. Starling, AIChE J. **18**, 1184 (1972).
[7] C. Kim, P. Vimalchand, M. Donohue, and S. Sandler, AIChE J. **32**, 1726 (1986).
[8] W. G. Chapman, K. E. Gubbins, G. Jackson, and M. Radosz, Fluid Phase Equilib. **52**, 31 (1989).
[9] W. G. Chapman, K. E. Gubbins, G. Jackson, and M. Radosz, Ind. Eng. Chem. Res. **29**, 1709 (1990).
[10] E. A. Muller and K. E. Gubbins, Ind. Eng. Chem. Res. **40**, 2193 (2001).
[11] A. Gil-Villegas, A. Galindo, P. Whitehead, S. Mills, and G. Jackson, J. Chem. Phys. **106**, 4168 (1997).
[12] A. Galindo, L. Davies, A. Gil-Villegas, and G. Jackson, Mol. Phys. **93**, 241 (1998).
[13] U. Deiters and I. Pegg, J. Chem. Phys. **90**, 6632 (1989).
[14] T. Kraska and U. Deiters, J. Chem. Phys. **96**, 539 (1992).
[15] A. van Pelt, C. Peters, and J. deSwaan Arons, J. Chem. Phys. **95**, 7569 (1991).
[16] C. McCabe, A. Galindo, A. Gil-Villegas, and G. Jackson, Int. J. Thermophys. **19**, 1511 (1998).
[17] C. McCabe, A. Gil-Villegas, and G. Jackson, J. Phys. Chem. B **102**, 4183 (1998).
[18] L. Sun, H. Zhao, S. Kiselev, and C. McCabe, J. Phys. Chem. B **109**, 9047 (2005).
[19] Y. Katayama, T. Mizutani, W. Utsumi, O. Shimomura, M. Yamakata, and K. Funakoshi, Nature (London) **403**, 170 (2000).
[20] R. Kurita and H. Tanaka, Science **306**, 845 (2004).
[21] R. Kurita and H. Tanaka, J. Phys.: Condens. Matter **17**, L93 (2005).
[22] S. Sastry and C. Angell, Nat. Mater. **2**, 739 (2003).
[23] T. Morishita, Phys. Rev. Lett. **93**, 055503 (2003).
[24] D. J. Lacks, Phys. Rev. Lett. **84**, 4629 (2000).
[25] I. Saika-Voivod, F. Sciortino, and P. H. Poole, Phys. Rev. E **63**, 011202 (2001).
[26] J. Gliosli and F. Ree, Phys. Rev. Lett. **82**, 4569 (1999).
[27] X. Wang, S. Scandolo, and R. Car, Phys. Rev. Lett. **95**, 185701 (2005).
[28] P. H. Poole, T. Grande, C. A. Angell, and P. F. McMillan, Science **275**, 322 (1997).
[29] J. L. Yarger and G. H. Wolf, Science **306**, 820 (2004).
[30] C. A. Angell, Annu. Rev. Phys. Chem. **55**, 559 (2004).
[31] P. G. Debenedetti, J. Phys.: Condens. Matter **15**, R1669 (2003).
[32] R. J. Speedy and C. A. Angell, J. Chem. Phys. **65**, 851 (1976).
[33] C. A. Angell, M. Oguni, and W. J. Sichina, J. Phys. Chem. **86**, 998 (1982).
[34] C. A. Angell, J. Shuppert, and J. C. Tucker, J. Phys. Chem. **77**, 3092 (1973).
[35] D. Rasmussen and A. Mackenzie, J. Chem. Phys. **59**, 5003 (1973).
[36] D. Rasmussen, A. Mackenzie, C. A. Angell, and J. C. Tucker, Science **181**, 342 (1973).
[37] E. Tombari, C. Ferrari, and G. Salvetti, Chem. Phys. Lett. **300**, 749 (1999).
[38] D. E. Hare and C. M. Sorensen, J. Chem. Phys. **84**, 5085 (1986).
[39] D. E. Hare and C. M. Sorensen, J. Chem. Phys. **87**, 4840 (1987).
[40] E. Burton and W. Oliver, Proc. R. Soc. London, Ser. A **153**, 166 (1935).
[41] O. Mishima, L. D. Calvert, and E. Whalley, Nature (London) **314**, 76 (1985).
[42] P. H. Poole, F. Sciortino, U. Essmann, and H. E. Stanley, Nature (London) **360**, 324 (1992).
[43] O. Mishima and H. E. Stanley, Nature (London) **392**, 164 (1998).
[44] O. Mishima, Phys. Rev. Lett. **85**, 334 (2000).
[45] F. H. Stillinger and A. Rahman, J. Chem. Phys. **57**, 1281 (1972).
[46] M. W. Mahoney and W. L. Jorgensen, J. Chem. Phys. **112**, 8910 (2000).
[47] S. Harrington, R. Zhang, P. H. Poole, F. Sciortino, and H. E. Stanley, Phys. Rev. Lett. **78**, 2409 (1997).
[48] P. H. Poole, I. Saika-Voivod, and F. Sciortino, J. Phys.: Condens. Matter **17**, L431 (2005).
[49] M. Yamada, H. E. Stanley, and F. Sciortino, Phys. Rev. E **67**, 010202 (2003).
[50] M. Yamada, S. Mossa, H. E. Stanley, and F. Sciortino, Phys. Rev. Lett. **88**, 195701 (2002).
[51] P. H. Poole, F. Sciortino, T. Grande, H. E. Stanley, and C. A. Angell, Phys. Rev. Lett. **73**, 1632 (1994).
[52] C. A. Jeffery and P. H. Austin, J. Chem. Phys. **110**, 484 (1999).
[53] T. M. Truskett, P. G. Debenedetti, S. Sastry, and S. Torquato, J. Chem. Phys. **111**, 2647 (1999).
[54] T. M. Truskett and K. A. Dill, J. Chem. Phys. **117**, 5101 (2002).
[55] T. M. Truskett and K. A. Dill, J. Phys. Chem. B **106**, 11829 (2002).
[56] I. Brovchenko, A. Geiger, and A. Oleinikova, J. Chem. Phys. **118**, 9473 (2003).
[57] I. Brovchenko, A. Geiger, and A. Oleinikova, J. Chem. Phys. **123**, 044515 (2005).
[58] J. P. Hansen and L. Verlet, Phys. Rev. **184**, 151 (1969).
[59] D. S. Corti and P. G. Debenedetti, Chem. Eng. Sci. **49**, 2717 (1994).
[60] T. Loerting, E. J. Saltzman, I. Kohl, E. Mayer, and A. Hallbrucker, Phys. Chem. Chem. Phys. **3**, 5355 (2001).
[61] R. Martonák, D. Donadio, and M. Parrinello, Phys. Rev. Lett. **92**, 225702 (2004).
[62] R. Martonák, D. Donadio, and M. Parrinello, J. Chem. Phys. **122**, 134501 (2005).
[63] N. Giovambattista, H. E. Stanley, and F. Sciortino, Phys. Rev. Lett. **94**, 107803 (2005).
[64] S. Sastry, P. G. Debenedetti, F. Sciortino, and H. E. Stanley, Phys. Rev. E **53**, 6144 (1996).
[65] L. P. Rebelo, P. G. Debenedetti, and S. Sastry, J. Chem. Phys. **109**, 626 (1998).
[66] O. Mishima, J. Chem. Phys. **123**, 154506 (2005).
[67] H. S. Ashbaugh, T. M. Truskett, and P. G. Debenedetti, J. Chem. Phys. **116**, 2907 (2002).
[68] S. Chatterjee, H. S. Ashbaugh, and P. G. Debenedetti, J. Chem. Phys. **123**, 164503 (2005).
[69] J. Tester and M. Modell, *Thermodynamics and its Applications*, 3rd ed. (Prentice-Hall, Upper Saddle River, NJ, 1997).
[70] M. A. Anisimov, E. E. Gorodetskii, V. D. Kulikov, and J. V. Sengers, Phys. Rev. E **51**, 1199 (1995).